

**UNCLASSIFIED**

**AD** **409 729**

**DEFENSE DOCUMENTATION CENTER**

**FOR**

**SCIENTIFIC AND TECHNICAL INFORMATION**

**CAMERON STATION, ALEXANDRIA, VIRGINIA**



**UNCLASSIFIED**

NOTICE: When government or other drawings, specifications or other data are used for any purpose other than in connection with a definitely related government procurement operation, the U. S. Government thereby incurs no responsibility, nor any obligation whatsoever; and the fact that the Government may have formulated, furnished, or in any way supplied the said drawings, specifications, or other data is not to be regarded by implication or otherwise as in any manner licensing the holder or any other person or corporation, or conveying any rights or permission to manufacture, use or sell any patented invention that may in any way be related thereto.

CATALOGED BY DDC 409729

409 729

AS AD No.

63-4-2

# DEFECTS IN ALUMINUM QUENCHED FROM THE LIQUID STATE

G. THOMAS AND R. H. WILLENS

MAY 1963

---

A REPORT ON RESEARCH CONDUCTED UNDER  
CONTRACT FOR THE U.S. ATOMIC ENERGY COM-  
MISSION AND THE OFFICE OF NAVAL RESEARCH

W. M. KECK LABORATORY OF  
ENGINEERING MATERIALS

CALIFORNIA INSTITUTE OF TECHNOLOGY  
PASADENA

California Institute of Technology  
W. M. Keck Laboratory of Engineering Materials

DEFECTS IN ALUMINUM QUENCHED FROM THE LIQUID STATE

by

G. Thomas and R. H. Willens

Technical Report No. 15 submitted to:

U. S. Atomic Energy Commission Contract No. AT(04-3)-221 and  
Office of Naval Research, Contract No. Nonr-220(30)

Approved by Pol Duwez  
Professor of Materials Science

May 1963

---

Reproduction in whole or in part is permitted for any purpose of the  
United States Government.

# ABSTRACT

High purity aluminum was quenched from the liquid state and specimens were examined by transmission electron microscopy. Very high densities of defects in the form of perfect loops, imperfect loops, and small black spots were observed. The vacancy concentration, as deduced from the number and size of defects, increase with increasing temperature at a much slower rate in the liquid than in the solid. Both the vacancy formation energy and the entropy factor appear to be considerably reduced above the melting point. Also, a discontinuity in the vacancy concentration is observed at the melting point.

## 1. INTRODUCTION

Previous experiments on the quenching-in of vacancies in metals have been limited to solid state quenching with cooling rates of the order of fifty thousand degrees per second. It is now well known that in quenched metals, vacancies condense out in various dislocation configurations, namely, perfect loops, imperfect loops, or tetrahedra, depending upon stacking fault energy, purity and vacancy supersaturation (see reviews in Refs. 1 and 2). The quenching-in of vacancies in high purity solid aluminum has been studied previously by resistivity<sup>(4,5)</sup>, transmission electron microscopy<sup>(6-8)</sup>, and simultaneous x-ray and dilatometry<sup>(9)</sup>. The vacancy concentration can be expressed as  $c = A \exp(-Q_f/kT)$  where, for aluminum,  $A = 8$  and  $Q_f = 0.76$  eV. At the melting point of aluminum ( $933^\circ\text{K}$ ), the vacancy concentration is  $6 \times 10^{-4}$ .

The method of rapid quenching from the melt, described by Duwez and Willens<sup>(3)</sup>, offers the possibility of investigating the quenching-in of vacancies from the liquid state. It has been estimated that the cooling rates achieved by this quenching technique are of the order of one or two million degrees per second. The experiments described in this paper are carried out on quenched liquid aluminum. Both the variations of vacancy concentration with quenching temperature and the type of vacancy defects that were formed have been investigated.

## 2. EXPERIMENTAL PROCEDURE

The aluminum used in this investigation had a purity of 99.996%, magnesium being the predominant impurity (30 ppm). The foils produced

by this quenching technique were non-uniform in thickness, the average thickness being of the order of several microns. However, there were regions within the foil which were thin enough to be viewed in transmission electron microscopy without any further thinning being necessary<sup>(10)</sup>. Only these regions were examined to determine the vacancy concentrations. In most cases, the foil was observed immediately after quenching without aging at elevated temperatures. Some foils were aged for several minutes between 100°C and 140°C. No difference in structure between the as-quenched foil and the aged foils was noticed except for some loop growth. The high concentration of vacancies which were retained by the quench resulted in the formation of Frank-sessile loops, perfect loops, and small dark spots which may be very small loops or vacancy clusters. The vacancy concentration was determined from the size and density of loops using the formula  $c = \pi r^2 b n / t$ , where  $n$  is the number of loops per  $\text{cm}^2$ ,  $r$  the loop radius,  $b$  the Burgess vector ( $a/3 \langle 111 \rangle$  for Frank loops,  $a/2 \langle 110 \rangle$  for perfect loops) and  $t$  the foil thickness. For the case of spherical clusters with radius  $r$ , this formula would underestimate the vacancy concentration by a factor of  $4r/3b$ . The actual foil thickness was of the order of  $3 \times 10^{-5}$  cm, however, a value of  $10^{-5}$  cm was adopted for the calculations in view of the fact that vacancy denudation occurs at both the top and bottom surfaces of the foil.

### 3. RESULTS

Typical electron micrographs from foils quenched from various temperatures above the melting point are shown in Figs. 1 to 6. Quenches from below 1200°C produce large numbers of loops or clusters.



Figure 1. Defect structure in aluminum quenched from  $1165^{\circ}\text{C}$  showing high density of loops and black spots.





Figure 2. Defect structure in aluminum quenched from 725°C. There is a narrow denuded zone between 500 and 1000 Å wide, next to grain boundaries.



Figure 3. Defect structure in aluminum quenched from 765°C. A zig zag dislocation has produced a loop-free area A.



Figure 4. Loops and black spots in a (111) area after quenching from  $1165^{\circ}\text{C}$ . Operating reflection  $(2\bar{2}0)$ . Notice absence of loops in the (111) plane showing they are all of the Frank-sessile kind ( $b = a/3 [111]$ ).



Figure 5. Small grain size in Al quenched from 900°C. By tilting the specimen, the loops in region A can be brought into contrast. Large perfect diamond-shaped loops are visible at B.

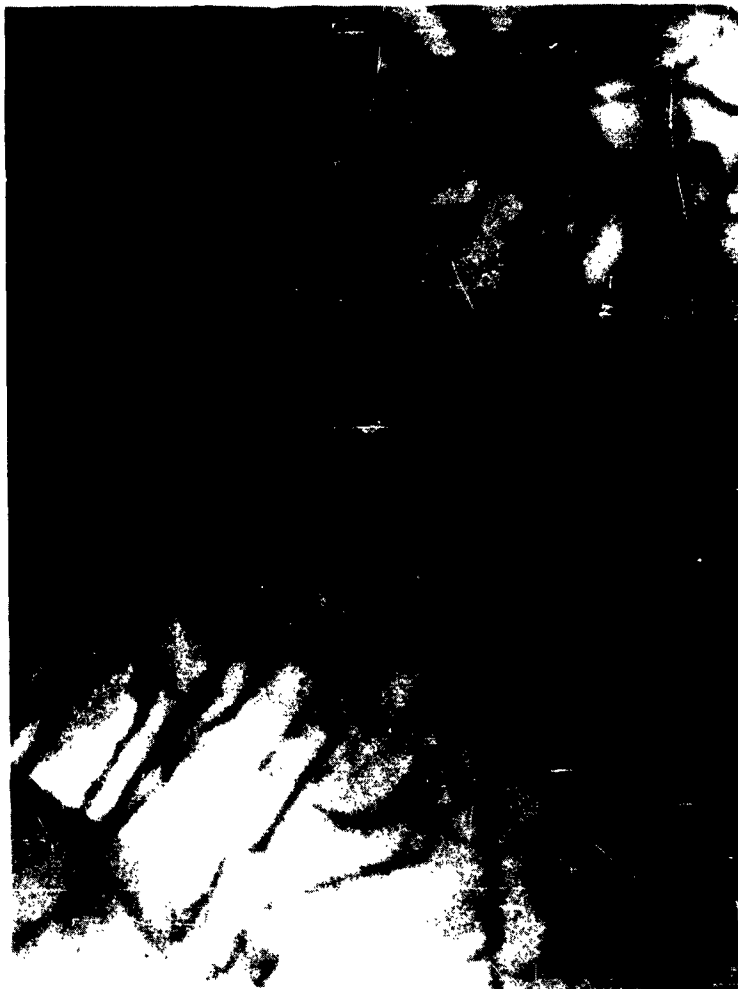


Figure 6. Aluminum quenched from 1260°C. Notice the absence of loops and the high density of dislocations making sub-boundaries.

At higher temperatures few loops are observed but the density of dislocations is very large (Fig. 6). Below  $1200^{\circ}\text{C}$  most of the dislocations appear to be in the form of loops except as shown at A in Fig. 3 where a zig zag dislocation line exists in a loop-free area. Apparently many dislocations are generated by quenching from temperatures greater than  $1200^{\circ}\text{C}$  and these effectively sweep up most of the retained vacancies. In addition, the quenching efficiency is probably reduced with increasing temperature of the melt due to the thermal capacity of the sample. Thus some vacancies will have time to escape from the thin regions of the foil during cooling. As shown in Figs. 1 and 2 very high densities of defects are observed after quenching from below  $1200^{\circ}\text{C}$ . The grain size is very small ( $1/4$  to  $1/4$ ) and the grains have nearly equilibrium shapes (Fig. 5). Another interesting feature is that the width of the vacancy denuded zone is between 500 and  $1500 \text{ \AA}$  which is much less than that observed in aluminum quenched from below the melting point ( $1/4$ ). This fact and the observed high densities of defects indicate that numerous vacancies have been quenched-in.

Perfect and imperfect dislocation loops have been resolved as well as small spherical black spots (Figs. 3 and 4) which could be small loops or vacancy clusters. These three types of defects are observed in specimens quenched from below  $1200^{\circ}\text{C}$ . Figure 4 is an example of an area in (111) orientation. Only three orientations of loops are visible corresponding to the traces of  $(\bar{1}\bar{1}1)$  ( $1\bar{1}\bar{1}$ ) and  $(11\bar{1})$  planes with the foil surface. Loops in the plane of the foil are not visible, indicating that the Burgers vector must be normal to the foil surface. This must mean that the loops are of the Frank kind since

perfect loops would have all four possible orientations visible in the (111) orientation. Most of the very small loops do appear to be Frank loops, but larger, perfect loops, many of which are diamond-shaped, are also observed (for instance at B, Fig. 5).

Table I gives the number of defects per  $\text{cm}^3$  and the average vacancy concentration calculated on the basis of perfect loop defects. These results are probably on the low side because 1/ not all of the vacancies may have condensed to the loops, 2/ not all loops may be visible because of contrast conditions (Fig. 5) and, 3/ many of the defects may be spherical clusters and the concentration calculations, which assume loops, would underestimate the concentration.

TABLE I

Quenching Temperature ( $^{\circ}\text{C}$ )	Treatment	Loop radius (A)	Number of Loops per $\text{cm}^3$	Average Vacancy Concentration $C \times 10^3$
725	As Cast	100	$1.3 \times 10^{16}$	1.04
820	2 Min. at $136^{\circ}\text{C}$	250-625	$1.6 \times 10^{15}$	1.34
1030	As Cast	100	$1.5 \times 10^{16}$	1.29
1165	As Cast	110	$1.4 \times 10^{16}$	1.60

A plot of  $\ln c$  against reciprocal temperature is shown in Fig. 7. It can be seen that there is a sharp change in slope and a discontinuity in vacancy concentration at the melting point. The equation of the line, representing quenches from the liquid, is  $c = 4 \times 10^{-3} \exp(-0.11/kT)$ .

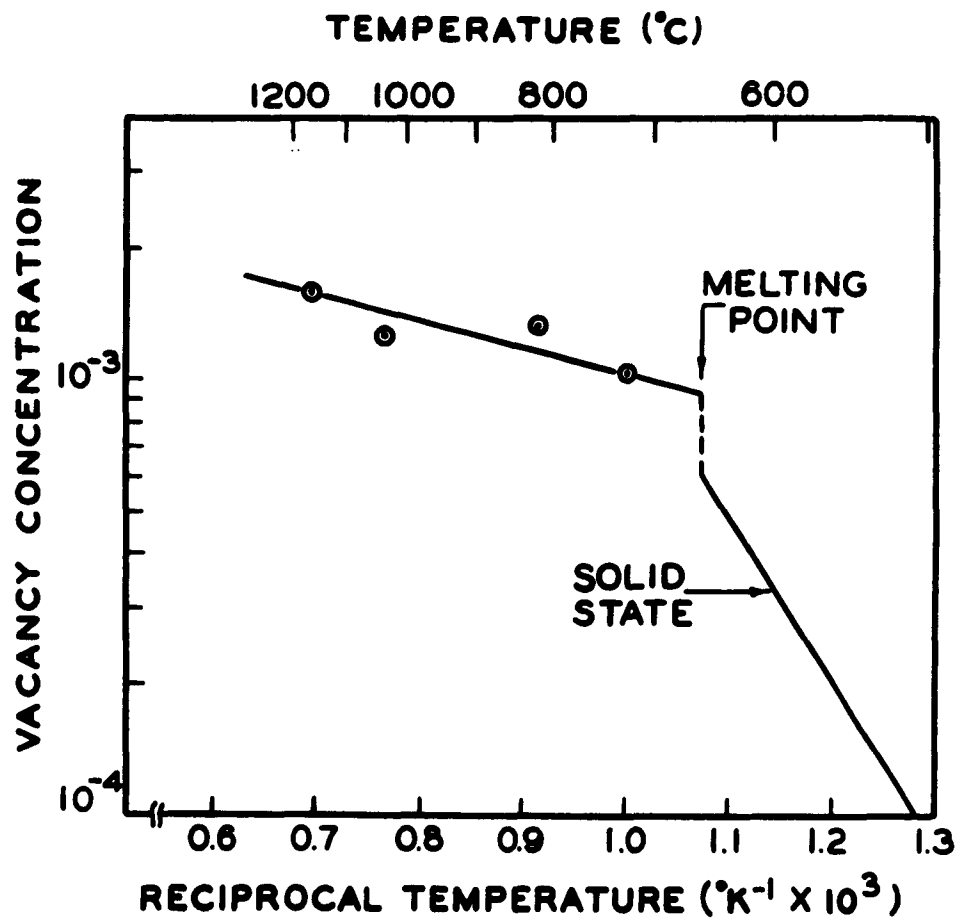


Figure 7. Relationship between vacancy concentration and reciprocal temperature. The solid state line is taken from the data of References 4 and 9.



## DISCUSSION

The very high and uniform densities of defects observed in these experiments indicate that very large supersaturations of vacancies are retained by rapid quenching from the liquid state. The appearance of three kinds of defects, namely, perfect loops, imperfect loops, and small black spots, is indicative of various stages in the annihilation of vacancies depending upon local conditions of vacancy supersaturation and quenching stresses. Another possibility is that the defects may form at the solid-liquid interface<sup>(15)</sup>. Previous calculations<sup>(16,17)</sup> show that stable vacancy clusters or loops trapped behind the interface would not diffuse back to the liquid due to the high interfacial velocity (estimated to be 10 cm/sec.). These calculations are slightly in error because no change in the vacancy formation energy between the liquid and solid states and no discontinuity in equilibrium vacancy concentration are assumed.

The increase in vacancy concentration at the melting point contributes to the entropy of melting. Assuming a random two-component system, the increase in entropy on melting due to a change in vacancy concentration is<sup>(11)</sup>

$$\frac{\Delta S}{Nk} = \left[ c_1 \ln c_1 - c_2 \ln c_2 + (1-c_1) \ln (1-c_1) - (1-c_2) \ln (1-c_2) \right] ,$$

where  $c_1$  is the vacancy concentration in the solid and  $c_2$  the vacancy concentration in the liquid. Using  $c_1 = 6 \times 10^{-4}$  and  $c_2 = 1 \times 10^{-3}$  at the melting point, the entropy change is  $2.9 Nk \times 10^{-3}$ . The total

entropy change on melting, as deduced from the heat of fusion, is 1.4 Nk for aluminum. Therefore, the entropy increase associated with the change in vacancy concentration is very small. The largest contribution to the entropy change is probably configurational entropy, since there is evidence that the vibrational frequencies, the only other source of entropy associated with melting, is not appreciably altered<sup>(12,13,14)</sup>.

Perhaps the most interesting results obtained in this investigation is that within the experimental limits of the electron microscopy technique, the vacancy concentration is relatively insensitive to temperatures above the melting point. The entropy factor and the formation energy of a vacancy are both smaller in the liquid than in the solid. The ratio is about three orders of magnitude in the entropy factor and about a factor of seven in the formation energy.

## REFERENCES

1. M. J. Whelan, Electron Microscopy and Strength of Crystals (Eds. G. Thomas and J. Washburn), Interscience, N. Y., p. 3 (1963).
2. G. Thomas and J. Washburn, Symposium on Point Defects, Dallas, Texas, 1963, to be published in Rev. Mod. Physics.
3. Pol Duwez and R. H. Willens, Trans. AIME, 227, 362 (1963).
4. F. J. Bradshaw and S. Pearson, Phil. Mag., 2, 379, 570 (1957).
5. C. Panzeri and T. Federighi, Phil. Mag. 3, 1223 (1958).
6. P. B. Hirsch, J. Silcox, R. E. Smallman and K. H. Westmacott, Phil. Mag., 3, 897 (1958).
7. D. Kuhlmann-Wilsdorf and H.G.F. Wilsdorf, J. Appl. Phys., 31, 516 (1960).
8. R. M. J. Cotterill and R. L. Segal, Proc. Fifth International Congress for Electron Microscopy, Philadelphia, Pa., Academic Press, N. Y., J-13 (1962).
9. R. O. Simmons and R. W. Balluffi, Phys. Rev., 117, 52 (1960).
10. R. H. Willens, Proc. Fifth International Congress for Electron Microscopy, Philadelphia, Pa., Academic Press, N. Y., EE-6 (1962).
11. A. H. Cottrell, Theoretical Structural Metallurgy, Arnold, London, p. 110 (1948).
12. P. A. Egelstaff, Brit. J. Appl. Phys., 10, 1 (1959).
13. I. Petah, W. L. Wittemore, and A. W. McReynolds, Phys. Rev., 113, 767 (1959).
14. B. N. Brockhouse and N. K. Pope, Phys. Rev. Letters, 3, 259 (1959).
15. B. Chalmers, Impurities and Imperfections, American Society for Metals, p. 84 (1955).
16. G. Shoeck and W. A. Tiller, Phil. Mag., 5, 43 (1960).
17. K. A. Jackson, Phil. Mag., 7, 1117 (1962).

# DISTRIBUTION LIST FOR CONTRACT Nonr 220(30)

A

<u>AGENCY</u>	<u>NUMBER OF COPIES</u>
Chief of Naval Research Department of the Navy Washington 25, D. C. Attention: Code 423	2
Commanding Officer Office of Naval Research Branch Office 346 Broadway New York 13, New York	1
Commanding Officer Office of Naval Research Branch Office 495 Summer Street Boston 10, Massachusetts	1
Commanding Officer Office of Naval Research Branch Office 86 E. Randolph Street Chicago 1, Illinois	1
Commanding Officer Office of Naval Research Branch Office 1030 E. Green Street Pasadena 1, California	1
Commanding Officer Office of Naval Research Branch Office 1000 Geary Street San Francisco 9, California	1
Assistant Naval Attache for Research Office of Naval Research Branch Office, London Navy 100, Box 39 F.P.O., N.Y., N.Y.	5
Director U. S. Naval Research Laboratory Washington 25, D. C. Attention: Technical Information Officer, Code 2000	6
: Code 2020	1
: Code 6200	1
: Code 6300	2
: Code 6100	1

AGENCYNUMBER OF COPIES

Chief, Bureau of Naval Weapons Department of the Navy Washington 25, D. C. Attention: Code RRMA	1
: Code RREN-6	1
Commanding Officer U. S. Naval Air Material Center Philadelphia, Pennsylvania Attention: Aeronautical Materials Laboratory	1
Chief, Bureau of Yards and Docks Department of the Navy Washington 25, D. C. Attention: Research and Standards Division	1
Commanding Officer U. S. Naval Ordnance Laboratory White Oaks, Maryland	1
Commanding Officer U. S. Naval Proving Ground Dahlgren, Virginia Attention: Laboratory Division	1
Chief, Bureau of Ships Department of the Navy Washington 25, D. C. Attention: Code 315	1
: Code 335	1
: Code 341	1
: Code 350	1
: Code 634	1
Commanding Officer U. S. Naval Engineering Experiment Station Annapolis, Maryland Attention: Metals Laboratory	1
Materials Laboratory New York Naval Shipyard Brooklyn 1, New York Attention: Code 907	1

<u>AGENCY</u>	<u>NUMBER OF COPIES</u>
Commanding Officer David Taylor Model Basin Washington 7, D. C.	1
Post Graduate School U. S. Naval Academy Monterey, California Attention: Department of Metallurgy	1
Office of Technical Services Department of Commerce Washington 25, D. C.	1
Commanding Officer U. S. Naval Ordnance Test Station Inyokern, California	1
Armed Services Technical Information Agency (ASTIA) Documents Service Center Arlington Hall Station Arlington, Va.	5
Commanding Officer Watertown Arsenal Watertown, Massachusetts Attention: Ordnance Materials Research Office	1
: Laboratory Division	1
Commanding Officer Office of Ordnance Research Box CM, Duke Station Duke University Durham, North Carolina Attention: Metallurgy Division	1
Commander Wright Air Development Center Wright-Patterson Air Force Base Dayton, Ohio Attention:	
: Aeronautical Research Lab. (WCRRL)	1
: Materials Laboratory (WCRTL)	1

AGENCYNUMBER OF COPIES

U. S. Air Force ARDC Office of Scientific Research Washington 25, D. C. Attention: Solid State Division (SRQB)	1
National Bureau of Standards Washington 25, D. C. Attention: Metallurgy Division	1
: Mineral Products Division	1
National Aeronautics Space Administration Lewis Flight Propulsion Laboratory Cleveland, Ohio Attention: Materials and Thermodynamics Division	1
U. S. Atomic Energy Commission Washington 25, D. C. Attention: Technical Library	1
U. S. Atomic Energy Commission Washington 25, D. C. Attention: Metals and Materials Branch	1
Division of Research	
: Eng. Develop. Branch	1
Division of Reactor Develop.	
Argonne National Laboratory P. O. Box 299 Lemont, Illinois Attention: H. D. Young, Librarian	1
Brookhaven National Laboratory Technical Information Division Upton, Long Island, New York Attention: Research Library	1
Union Carbide Nuclear Co. Oak Ridge National Laboratory P. O. Box P Oak Ridge, Tennessee Attention: Metallurgy Division	1
: Solid State Physics Division	1
: Laboratory Records Dept.	1

## E

AGENCYNUMBER OF COPIES

Los Alamos Scientific Laboratory P. O. Box 1663 Los Alamos, New Mexico Attention: Report Librarian	1
General Electric Company P. O. Box 100 Richland, Washington Attention: Technical Information Division	1
Iowa State College P. O. Box 14A, Station A Ames, Iowa Attention: F. H. Spedding	1
Knolls Atomic Power Laboratory P. O. Box 1072 Schenectady, New York Attention: Document Librarian	1
Sandia Corporation Sandia Base Albuquerque, New Mexico Attention: Library	1
U. S. Atomic Energy Commission Technical Information Service Extension P. O. Box 62 Oak Ridge, Tennessee Attention: Reference Branch	1
University of California Radiation Laboratory Information Division Room 128, Building 50 Berkeley, California Attention: R. K. Wakerling	1
Bettis Plant U. S. Atomic Energy Commission Bettis Field P. O. Box 1468 Pittsburgh 30, Pennsylvania Attention: Mrs. Virginia Sternberg, Librarian	1



AGENCYNUMBER OF COPIES

Commanding Officer and Director U. S. Naval Civil Engineering Laboratory Port Hueneme, California	1
Commanding Officer U. S. Naval Ordnance Underwater Station Newport, Rhode Island	1
U. S. Bureau of Mines Washington 25, D. C. Attention: Mr. J. B. Rosenbaum, Chief Metallurgist	1
Defense Metals Information Center Battelle Memorial Institute 505 King Avenue Columbus, Ohio	2
Solid State Devices Branch Evans Signal Laboratory U. S. Army Signal Engineering Laboratories c/o Senior Navy Liaison Officer U. S. Navy Electronic Office Fort Monmouth, New Jersey	1
U. S. Bureau of Mines P. O. Drawer B Boulder City, Nevada Attention: Electro-Metallurgical Div.	1
Commanding General U. S. Army Ordnance Arsenal, Frankford Philadelphia 37, Pennsylvania Attention: Mr. Harold Markus ORDBA-1320, 64-4	1
Picatinny Arsenal Box 31 Dover, New Jersey Attention: Lt. Hecht	1

<u>AGENCY</u>	<u>NUMBER OF COPIES</u>
Professor M. Cohen Department of Metallurgy Massachusetts Institute of Technology Cambridge 39, Massachusetts	1
Professor B. L. Averbach Department of Metallurgy Massachusetts Institute of Technology Cambridge 39, Massachusetts	1
Professor G. M. Pound Department of Metallurgical Engineering Carnegie Institute of Technology Pittsburgh 13, Pennsylvania	1
Professor B. E. Warren Department of Metallurgy Massachusetts Institute of Technology Cambridge 39, Massachusetts	1
Professor R. F. Hehemann Department of Metallurgical Engineering Case Institute of Technology Cleveland, Ohio	1
Professor G. C. Kuczynski Department of Metallurgy University of Notre Dame Notre Dame, Indiana	1
Professor J. M. Sivertsen Department of Metallurgy University of Minnesota Minneapolis, Minnesota	1
Professor V. G. Macres Department of Metallurgical Engineering Stanford University Stanford, California	1
Professor L. V. Azaroff Department of Metallurgical Engineering Illinois Institute of Technology Chicago 16, Illinois	1
Professor F. Seitz Department of Physics University of Illinois Urbana, Illinois	1

AGENCYNUMBER OF COPIES

Professor T. A. Read Department of Mining & Met. Engrg. University of Illinois Urbana, Illinois	1
Professor R. Smoluchowski Department of Mechanical Engineering Princeton University Princeton, New Jersey	1
Professor H. Brooks Dean of Graduate School of Applied Science Harvard University Cambridge, Massachusetts	1
Professor C. E. Birchenall Princeton University Princeton, New Jersey	1
Professor W. E. Wallace Department of Chemistry University of Pittsburgh Pittsburgh, Pennsylvania	1
Professor E. R. Parker Division of Mineral Technology University of California Berkeley 4, California	1
Professor L. G. Parratt Department of Physics Cornell University Ithaca, New York	1
Professor P. A. Beck Department of Mining and Metallurgy University of Illinois Urbana, Illinois	1
Professor P. Gordon Department of Metallurgical Engineering Illinois Institute of Technology Chicago 16, Illinois	1
Professor J. T. Norton Massachusetts Institute of Technology Department of Metallurgy Cambridge 39, Massachusetts	1

AGENCYNUMBER OF COPIES

Professor M. E. Nicholson  
Department of Metallurgy  
University of Minnesota  
Minneapolis 14, Minnesota

1

Professor J. W. Spretnak  
Department of Metallurgy  
Ohio State University  
Columbus, Ohio

1

Professor C. H. Shaw  
Department of Physics  
Ohio State University  
Columbus, Ohio

1

Professor F. R. Brotzen  
Department of Mechanical Engineering  
The Rice Institute  
Houston, Texas

1

Professor S. Weissman  
Materials Research Laboratory  
Rutgers University  
New Brunswick, New Jersey

1